Fermilab Library
0 1160 0052530 7

SDC-90-00145

SDC
SOLENOIDAL DETECTOR NOTES

RESOLUTION AND HERMETICITY OF THE LIQUID ARGON ELECTROMAGNETIC CALORIMETER AS A FUNCTION OF PSEUDORAPIDITY

C. Hearty

November, 1990

SDC-90-00145-REV
January 1991

Resolution and Hermeticity of the Liquid Argon Electromagnetic Calorimeter as a function of Pseudorapidity

Christopher Hearty
Lawrence Berkeley Laboratory

EGS has been used to calculate the electromagnetic energy resolution of a liquid argon calorimeter for $1 \leq E \leq 200$ GeV at $\eta = 0$, and for $E_t = 50$ GeV and 20 GeV at various angles in the barrel and across the barrel-endcap overlap. After corrections with massless gaps, 98.3% of the solid angle $0 < \eta < 3$ has a stochastic resolution $a < 0.25$.

1. Geometry

The geometry of the model is based on the liquid argon vessel quadrant drawing of Oct. 22, 1990. The details of the simulation, including wall thicknesses and locations, and the presence of polyethylene in the barrel section, agree with this drawing, except that all walls are flat, not curved (Figure 1). Because the EM sections are radially thin, the differences due to the curved surfaces are small. The amount of dead material in the overlap region agrees with a GEANT calculation that uses the complete geometry (Figure 2). The disagreement at $\eta = 1.52$ is due to differences in the internal details of the coil. Of the $1.9X_0$ at $\eta = 0$, 1.23 is due to the coil.

Module walls and gaps and the structural washers are not included. The barrel and endcap EM sections consist of a 1 cm thick strongback, a massless gap (mgap), and 35 active layers. The mgap is 2 mm LAr, 1.5 mm G-10 and 2 mm LAr. Each active layer is 4 mm pb, 2 mm LAr, 1.5 mm G-10 and 2 mm LAr. All structural members are aluminum. A third massless gap is located at the end of the barrel calorimeter, adjacent to the polyethylene. (It is perpendicular to the

One hundred showers were generated for each case. The energy deposited in each object (for example, a wall, LAr layer, or G-10 layer) was recorded for each shower.

2. Massless Gap Correction

The energy deposited in the massless gap layer is scaled by an energy and angle dependent scale factor to correct for the energy deposited in dead material before the calorimeter. In cases where there is significant energy deposited in only one, not both, of the barrel and endcap sections, the total deposited energy is:

$$E_{sum} = E_{LAr} + \alpha_{mg} E_{mg}, \tag{1}$$

where E_{LAr} is the energy deposited in the 35 active LAr layers, E_{mg} is the energy deposited in the massless gap, and α_{mg} is the massless gap correction scale factor. For no mgap correction, $\alpha_{mg} = 1$. α_{mg} is calculated from the 100 showers at each angle:

$$\alpha_{mg} = \frac{(E_0 - E_{leak}) \cdot s - E_{LAr}}{E_{mg}}, \tag{2}$$

where $s = 0.0896$ is the sampling fraction predicted by EGS. The value of α_{mg} ranges from 1 to 8 for the cases studied. The definition of α_{mg} ensures that the response of the detector is linear.

For $1.24 < \eta < 1.32$, there is significant energy deposited in all three of the massless gaps. Each mgap has a scale factor. For the third mgap,

$$\alpha^p_{mg} = \frac{(E^p_{mg} + E_{poly}) \cdot s}{E^p_{mg}}, \tag{3}$$

where E_{poly} is the energy deposited in the polyethylene. Of the other two mgaps, the correction factor for the mgap with the lower energy is

$$\alpha^l_{mg} = \frac{(E^l_{mg} + E^l_{dead}) \cdot s}{E^l_{mg}}, \tag{4}$$

where E^l_{dead} is the energy lost in the dead material before the barrel mgap or

between the barrel and endcap mgaps. For the higher energy mgap,

$$\alpha^h_{mg} = \frac{(E_0 - E_{leak}) \cdot s - E_{LAr} - \alpha^l_{mg} E^l_{mg} - \alpha^p_{mg} E_{poly}}{E^h_{mg}}. \tag{5}$$

The total energy is then

$$E_{sum} = E_{LAr} + \alpha^l_{mg} E^l_{mg} + \alpha^h_{mg} E^h_{mg} + \alpha^p_{mg} E_{poly}. \tag{6}$$

E_{LAr} is either the barrel, the endcap, or barrel plus endcap liquid argon energy, depending on the angle.

3. Energy Resolution at $\eta = 0$

Showers were generated at incident energies of 1, 2, 5, 10, 20, 50, 100, and 200 GeV. The energy deposited in each 10 cm square region — representing approximately 0.05 by 0.05 towers — was recorded for each LAr layer. The results are based on sums over a 5 by 5 or a 3 by 3 array of towers.

The stochastic resolution is plotted as a function of energy, with and without mgap correction, in Figure 3. With mgap correction, the data for energies greater and or equal to 5 GeV are consistent with a resolution of 0.11 +/- 0.01. These values were found using a Gaussian fit to E_{sum}; results using the mean and rms of the distribution differed by much less than the size of the error bars.

The resolution calculated using a 3 by 3 sum, with electronic noise, is unchanged with noise levels appropriate for preamps in the LAr. For preamps outside of the cryostat, the larger electronic noise slightly degrades the resolution at lower energies ($E \leq 20$ GeV).

The linearity of the calorimeter is represented by a plot of E_{sum} (with no mgap correction) divided by incident energy as a function of energy (Figure 4). There is no evidence for any nonlinearity above 100 GeV. This does not indicate that there are no mgap or leakage corrections at high energies — it indicates that the corrections are approximately constant with energy for this range of energies. (For both 100 and 200 GeV the corrections total 1%).

4. Energy Resolution as a Function of η

The E_t resolution at each angle is calculated at $E_t = 50$ GeV (and, in some cases, at $E_t = 20$ GeV) using the mean and rms of E_{sum}. The stochastic term a, assuming $\sigma_{E_t}/E_t = a/\sqrt{E_t}$, is plotted vs η, with and without mgap corrections, in Figure 5. In Figure 5(b), the dashed line displays the expected variation of a with angle due to the changing incident energy and effective plate thickness: $a = a_0$ in the barrel region and $a = a_0\sqrt{\tan\theta}$ in the endcap. Plotted is $a_0 = 0.11$; the data indicate that $a_0 = 0.110 \pm 0.004$. The solid line is an interpolation based on the amount of dead material before the LAr. The resolution in $1.44 < \eta < 1.62$ depends on the distribution of material in the coil, but is in the range $0.07 < a < 0.14$.

Figure 6 demonstrates that the third mgap following the polyethylene substantially improves the resolution at the boundary between the barrel calorimeter and the polyethylene, but otherwise has no effect.

The resolution for $E_t = 20$ GeV is shown in figure 7. The stochastic term is somewhat worse in regions with substantial amounts of dead material before the Lar.

After massless gap correction, 98.3% of the solid angle has E_t resolution $a < 0.25$, while 95% has $a < 0.18$. The mgaps also ensure that the response of the calorimeter at high energies is linear.

FIGURE CAPTIONS

1) Structural supports included in the EGS model. The cutout corner of the barrel calorimeter ($1.25 < \eta < 1.32$) is filled with polyethylene. The coil is made of aluminum at relative density 0.313. The dotted lines are some of the angles for which the resolution has been studied.

2) Dead material (X_0) before the active region of the calorimeter, as calculated by GEANT (histogram) and EGS (points). For $1.25 < \eta < 1.32$, the first massless gap is after approximately $4X_0$.

3) Electromagnetic resolution vs incident electron energy at $\eta = 0$, (a) with no massless gap correction, (b) with massless gap correction.

4) Fraction of total energy deposited in the liquid argon vs incident energy at $\eta = 0$, with no massless gap correction.

5) E_t resolution of the liquid argon EM calorimeter as a function of η, for $E_t = 50$ GeV; (a) no massless gap corrections; (b) including massless gap corrections.

6) Effect of the massless gap following the polyethylene; diamonds are resolution with the mgap, squares are resolution without.

7) E_t resolution for $E_t = 20$ GeV. The solid and dashed lines give the resolution curve for $E_t = 50$ GeV.

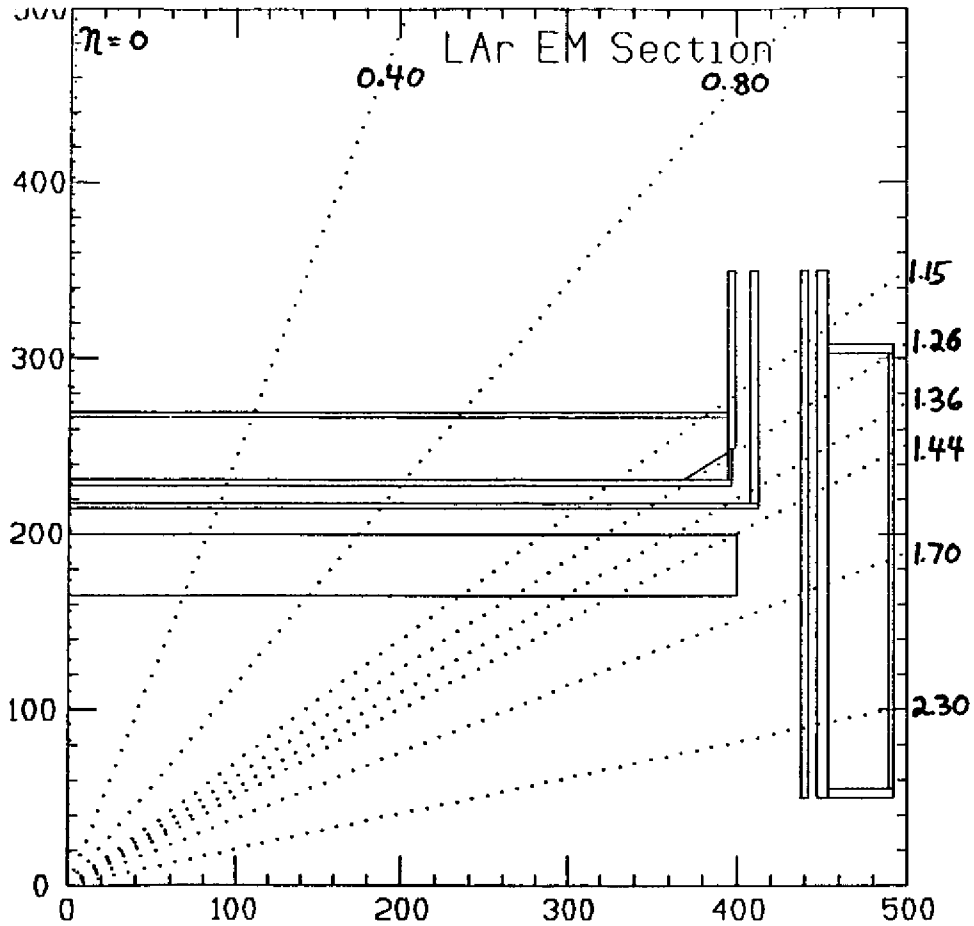

Figure 1

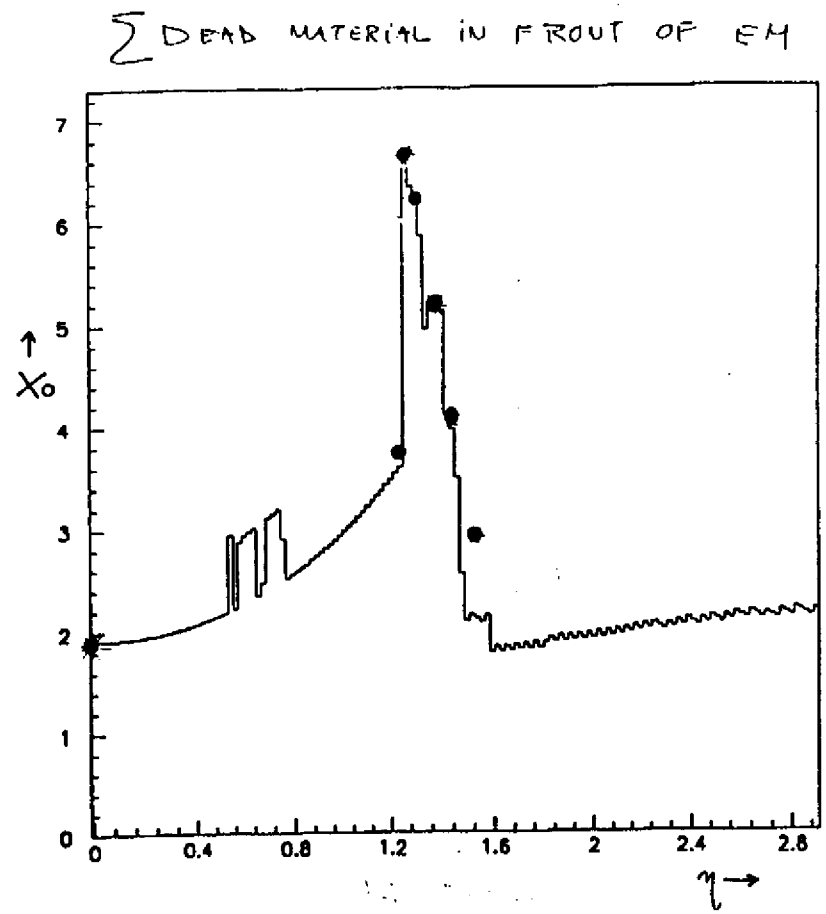

Figure 2

Resolution without Mgap Correction

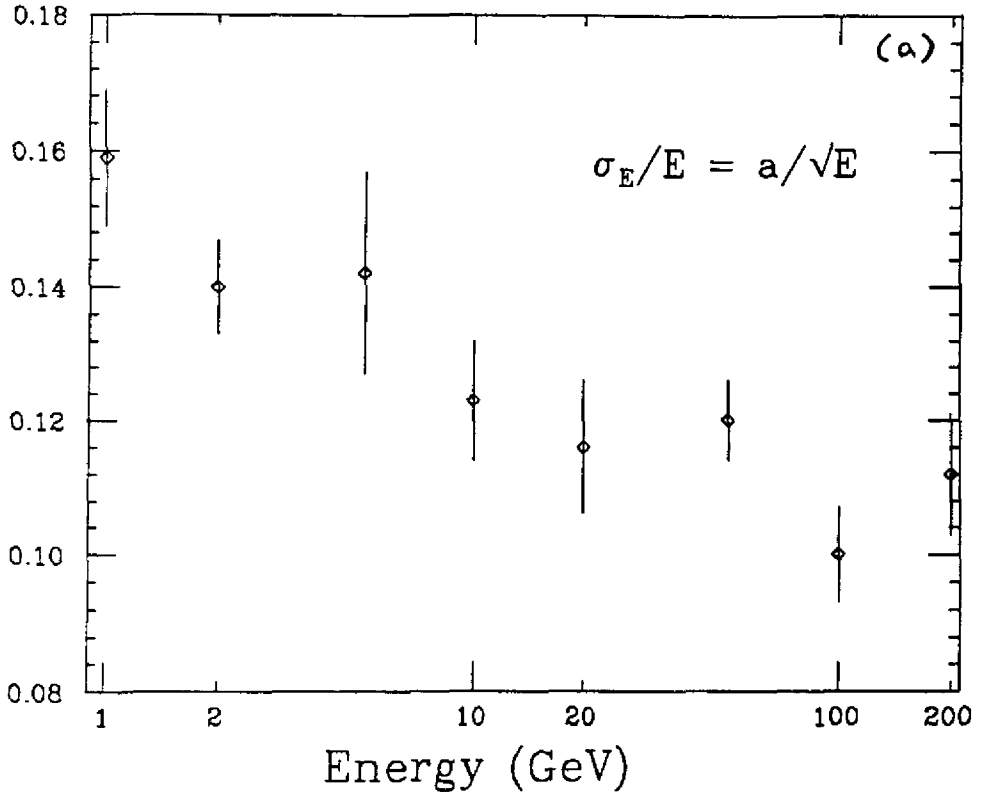

Figure 3a

Resolution with Mgap Correction

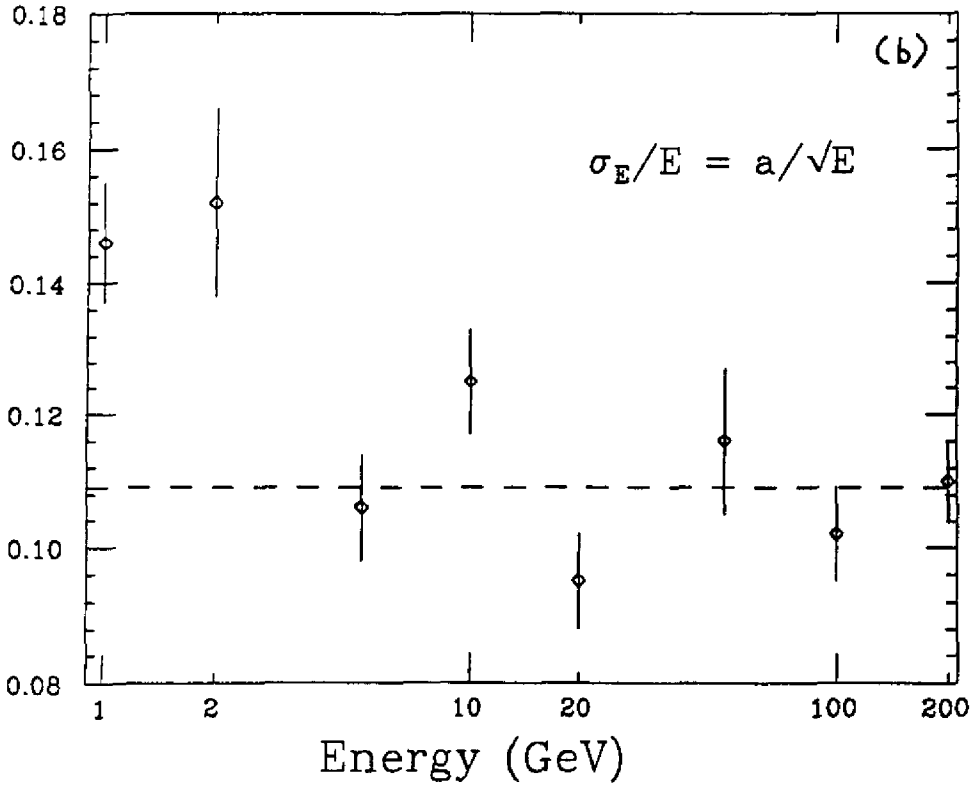

Figure 3b

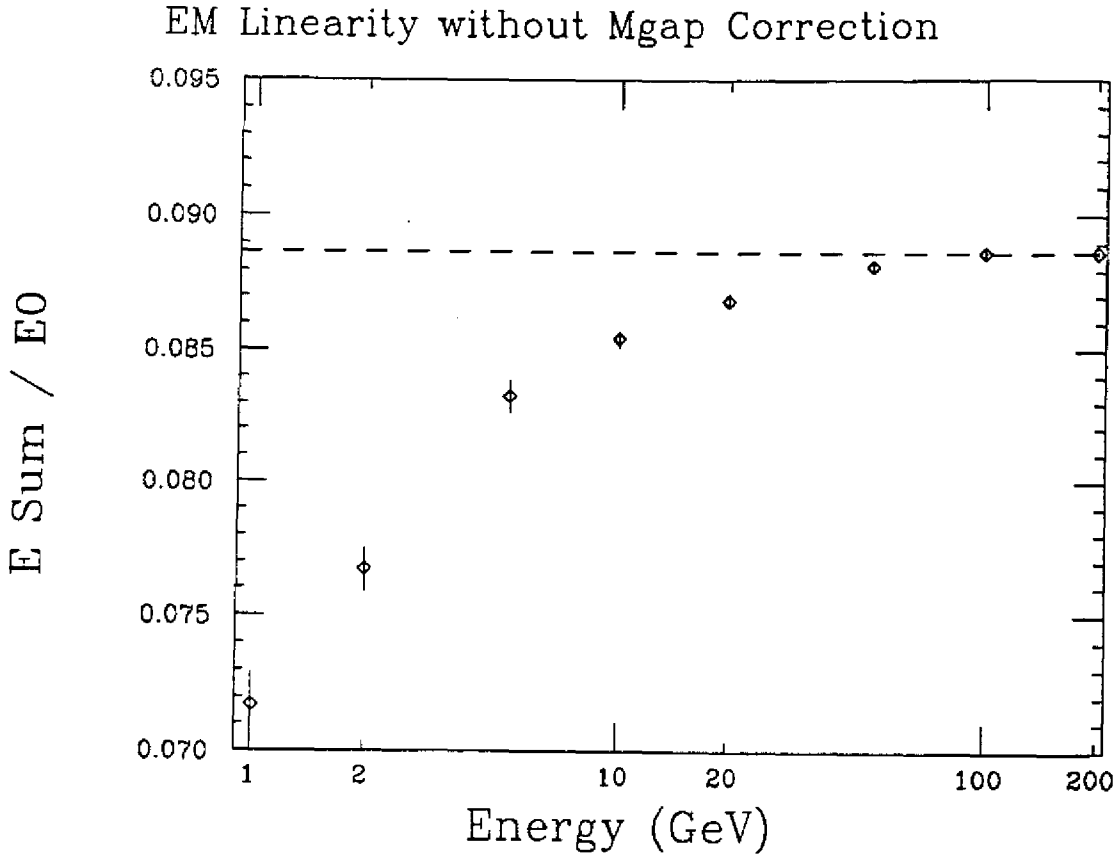

Figure 4

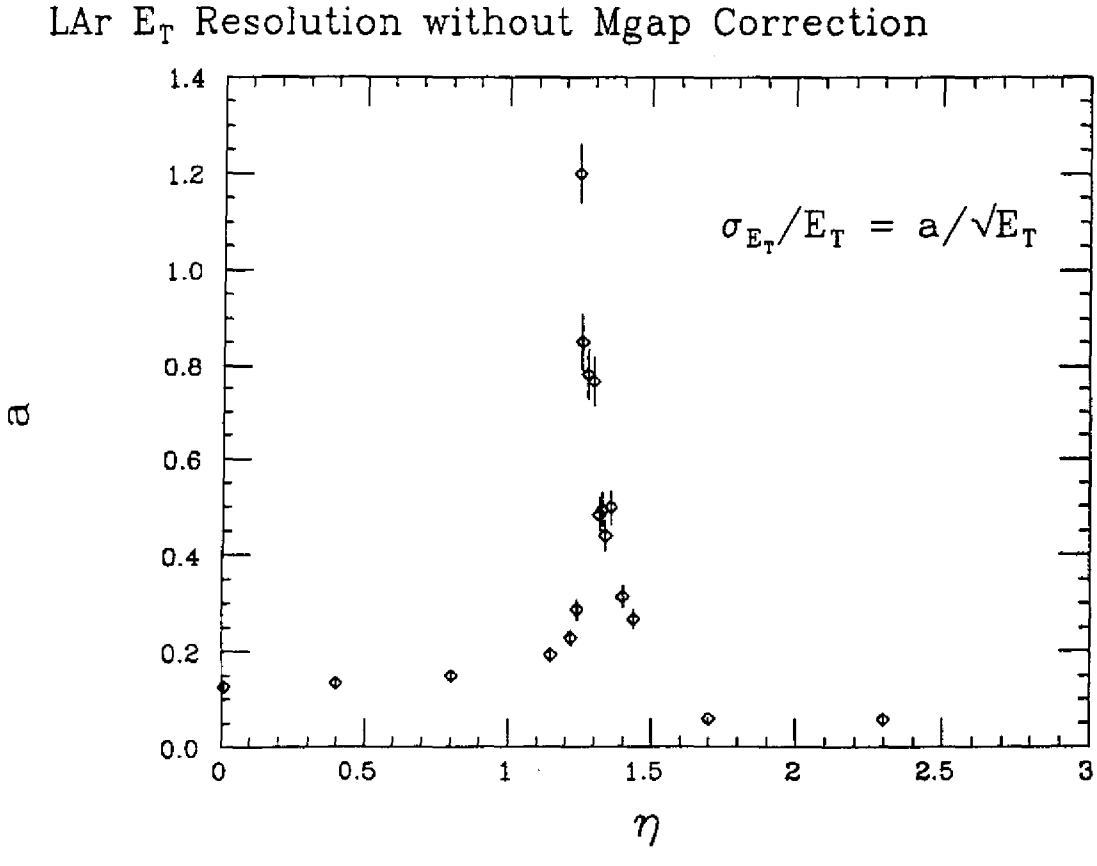

Figure 5a

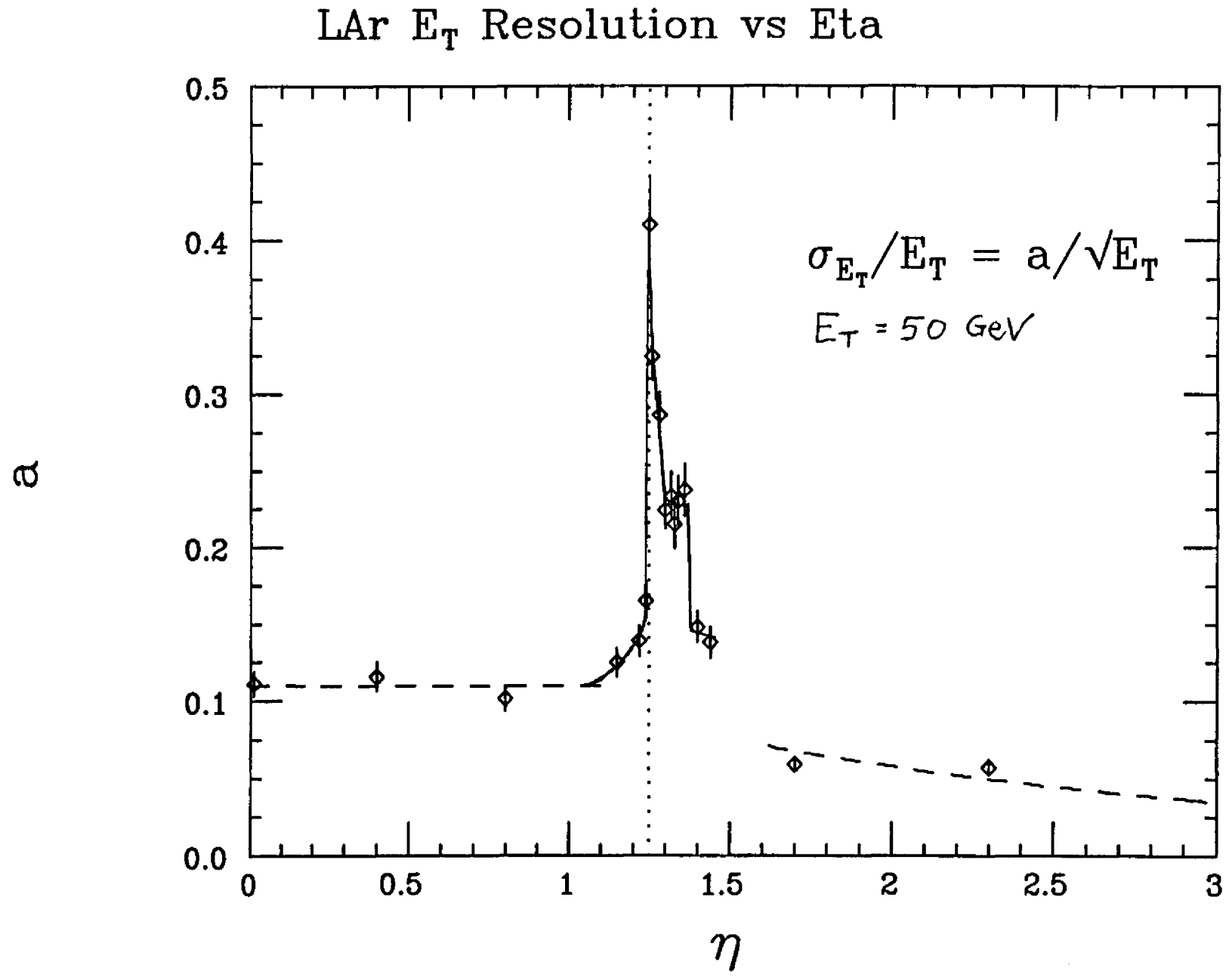
LAr E_T Resolution vs Eta
$\sigma_{E_T}/E_T = a/\sqrt{E_T}$
E_T = 50 GeV
a
η
0.0
0.1
0.2
0.3
0.4
0.5
0
0.5
1
1.5
2
2.5
3

Figure 5b

Resolution with and without Third Massless Gap

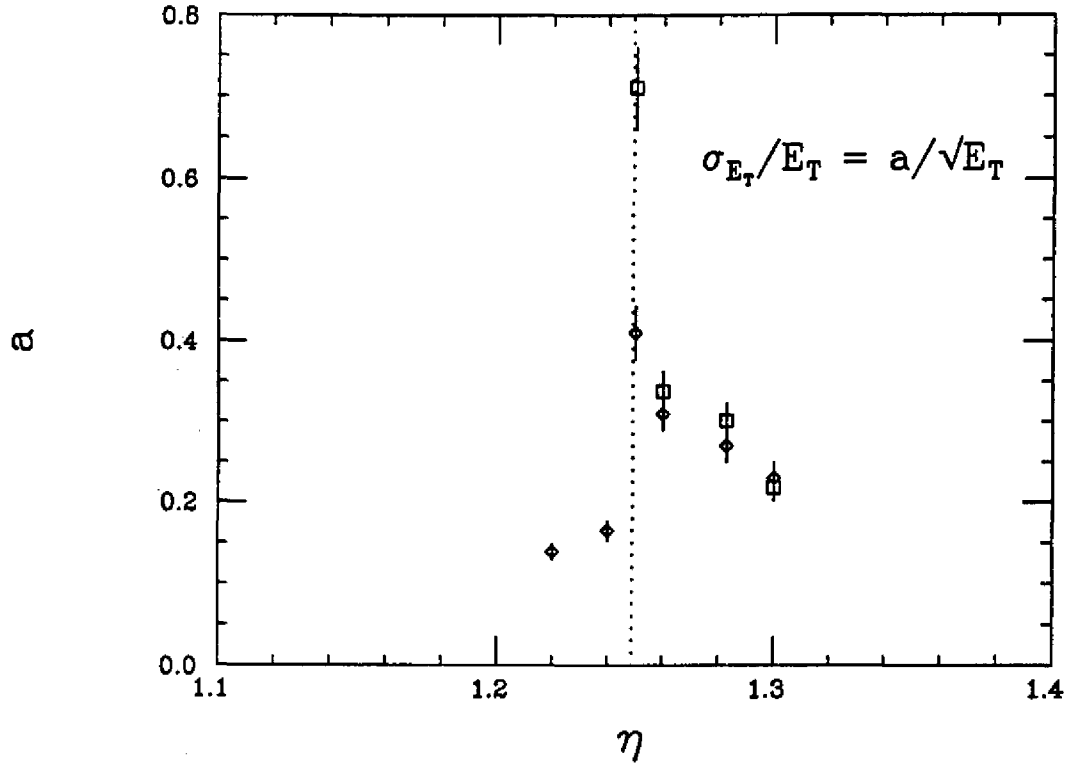

Figure 6

E_T Resolution, E_T=20 GeV

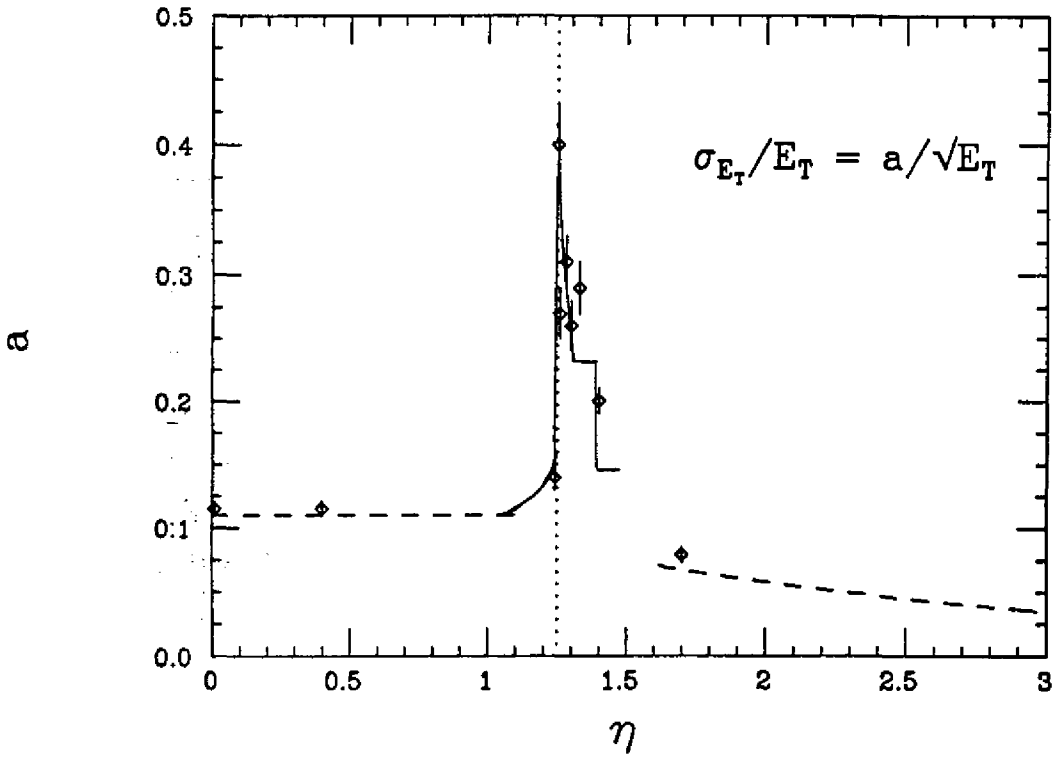

Figure 7